ELSEVIER

Inorganica Chimica Acta 290 (1999) 21–27

Inorganica Chimica Acta

Synthesis and characterization of a ferric complex of the tripodal ligand tris(2-benzimidazolylmethyl)amine—a superoxide dismutase mimic

Byunghoon Kwak [a], Ki Woong Cho [b], Myungho Pyo [c], Myoung Soo Lah [a,*]

[a] *Department of Chemistry, College of Science, Hanyang University, 1271 Sa-1-dong, Ansan, Kyunggi-do 425-170, South Korea*
[b] *Marine Natural Products Laboratory, Korea Ocean Research & Development Institute, Ansan, PO Box 29, Kyunggi-do 425-600, South Korea*
[c] *Department of Chemistry, College of Natural Science, Soonchun National University, Soonchun 540-742, South Korea*

Received 12 November 1998; accepted 23 February 1999

Abstract

The mononuclear iron complex **1** was synthesized using a tripodal ligand, tris(2-benzimidazolylmethyl)amine (ntb), where ntb served as a neutral tetradentate chelating ligand for the distorted octahedral ferric ion. Three benzimidazole groups of ntb and one chloride anion formed a base of octahedral geometry. One of the two axial positions was occupied by an apical nitrogen atom of ntb and the other site was occupied by another chloride anion. Two of the chloride anions in complex **1** are in a *cis* arrangement. The decay of the electrochemically generated superoxide radical (O_2^-) by complex **1** was observed using cyclic voltammetry. The superoxide dismutase (SOD) activity of complex **1** was also examined using a modified method of the light- and riboflavin-driven hydroxylaminenitrate assay. Reaction of complex **1** with an O_2^- radical in methanol gave the μ-oxo dinuclear iron complex **2**. The μ-oxo group was substituted for the basal chloride anion of complex **1** in complex **2**. Complex **2** could also be synthesized using weak bases instead of the O_2^- radical.

Keywords: Iron complexes; Tripodal amine complexes; Superoxide radical; Superoxide dismutase

1. Introduction

Superoxide dismutases (SODs) are metalloenzymes that disproportionate superoxide radicals, toxic byproducts of cellular respiration, to molecular oxygen and hydrogen peroxide [1]. Many low molecular weight biomimetic molecules have been proposed as SOD mimics, the vast majority of them being Cu–Zn–SOD mimics [2]. Recently, iron [3] and manganese [4] based SOD mimics have been reported. The most successful mimics were obtained using macrocyclic pentadentate ligands [3a,4a,b]. However, these structures are quite different from the distorted trigonal bipyramidal geometry of the active site structure of Mn- and Fe-SODs [5]. Nishida et al. claimed that the manganese and iron SOD mimics containing a tripodal tetradentate ligand, ntb, have SOD activity [4h]. However, we could not find any evidence of SOD activity in the manganese complex $[Mn(ntb)Cl]ClO_4$ [6]. In this study, we synthesized and characterized a mononuclear high spin ferric complex with a tripodal ligand, ntb, and its reactivity towards superoxide radicals was reinvestigated by an electrochemical study.

2. Experimental

2.1. Materials

The following were used as received with no further purification: tris(2-benzimidazolylmethyl)amine (ntb), potassium superoxide, sodium perchlorate, ferric chloride hexahydrate, sodium acetate, hexamethylene diamine and DMSO-d_6 from Aldrich; tetraethylammonium tetrafluoroborate ($TEABF_4$,) from Fluka;

* Corresponding author. Tel.: +82-345-400 5496; fax: +82-345-407 3863.

0020-1693/99/$ - see front matter
PII: S0020-1693(99)00091-2

methanol, ethanol, dimethylformamide, diethyl ether, chloroform, hexane and acetone from Carlo Erba; flavin mononucleotide (FMN), hydroxylamine, Tris base, Tris–HCl, EDTA, sulfanilic acid and naphthyl amine from Sigma Chemicals. FMN was further purified with DEAE-cellulose ion exchange column chromatography to remove contaminated riboflavin and stocked in 1 ml aliquots in a freezer at a concentration of 5 mM.

2.2. Instrumentation

C, H, N and Fe determinations were performed by the Elemental Analysis Laboratory of the Korean Institute of Basic Science. IR spectra were recorded as KBr pellets in the range 4000–600 cm^{-1} on a Bio-Rad FT-IR spectrometer. Absorption spectra were obtained using Perkin–Elmer Lambda spectrometer and a Bio-Rad microplate reader (model 3550). NMR spectra were obtained using a Varian-300 spectrometer. Positive-ion FAB mass spectra were obtained using a Jeol HX110A/HX110A tandem mass spectrometer in a glycerol matrix. Room temperature (r.t.) magnetic susceptibilities of well-ground solid samples were measured using an Evans balance. The measurements were calibrated against a $Hg[Co(SCN)_4]$ standard.

2.3. Synthesis

2.3.1. $[Fe(ntb)Cl_2]ClO_4$ (1)

A 1.00 g (2.50 mmol) sample of ntb was dissolved in 80 ml of methanol. When 0.663 g (2.50 mmol) of ferric chloride hexahydrate was added to the solution, a precipitate formed immediately. After 1 h of stirring, the solution was filtered. 1.27 g of the powder obtained was added to 100 ml of methanol and then 1.60 g (12.0 mmol) of sodium perchlorate was added to the resulting solution. After 1 h of stirring the solution was filtered. A red powder was again obtained (1.22 g, 80.0% yield). Slow evaporation of the filtrate solution over a 4 day period gave red crystals. The IR spectrum of the crystal was identical to that of the red powder sample. *Anal.* Calc. for $[Fe(ntb)Cl_2]ClO_4 \cdot H_2O$ ($FeC_{24}H_{23}N_7O_5Cl_3$) ($F_W = 632$): C, 44.23; H, 3.56; N, 15.04; Fe, 8.57. Found: C, 44.47; H, 4.37; N, 15.04; Fe, 8.63%. ^1H NMR (DMSO-d_6): δ 28.0, 44.2, 64.2. FABMS: m/z of $[Fe(ntb)Cl_2–HCl]^+$, 498. UV–Vis (MeOH) [λ_{max} (ε)]: 239 nm (6300 M^{-1} cm^{-1}), 272 nm (8000 M^{-1} cm^{-1}), 279 nm (8000 M^{-1} cm^{-1}), 305 nm (2400 M^{-1} cm^{-1}), 395 nm (1900 M^{-1} cm^{-1}). μ_{eff}: 6.02 μ_B.

2.3.2. $[Fe_2O(ntb)_2Cl_2](ClO_4)_2$ (2)

Method A: 0.787 g (1.24 mmol) of **1** was dissolved in 30 ml of methanol and 0.09 g (1.3 mmol) of KO_2 was dissolved in 10 ml methanol in another flask. The two solutions were mixed and stirred for 20 min and filtered. On standing for 1 week, red crystals were obtained in the filtrate (0.62 g, 94.2% yield).

Method B: 0.787 g (1.24 mmol) of **1** was dissolved in 30 ml of methanol and 0.12 g (1.5 mmol) of sodium acetate was added to the solution. After 30 min of stirring, the solution turned a clear red. Slow evaporation of the solution in a refrigerator gave red crystals (0.657 g, 97.8% yield).

Method C: 0.310 g (0.50 mmol) of **1** was dissolved in 20 ml of methanol and 0.025 g (0.25 mmol) of hexamethylene diamine was added to the solution. After 1 h of stirring, the solution was filtered (0.20 g, 74% yield). Slow evaporation of the filtrate solution gave red crystals (0.05 g, 20% yield). *Anal.* Calc. for $[Fe_2O(ntb)_2Cl_2](ClO_4)_2$ ($Fe_2C_{48}H_{42}N_{14}O_9Cl_4$): C, 47.55; H, 3.49; N, 16.17; Fe, 9.21. Found: C, 46.94; H, 4.06; N, 16.46; Fe, 8.80%. μ_{eff}: 2.0 μ_B. IR (KBr pellet): 790 cm^{-1} (for $Fe–O–Fe_{asym}$).

2.4. X-ray crystallography

Because a crystal of complex **1** loses its solvents of crystallization within 1 min, it was mounted in a glass capillary with the mother liquor to prevent the loss of the structural solvents during data collection. Preliminary examination and data collection were performed with Mo Kα radiation ($\lambda = 0.71069$ Å) on an Enraf-Nonius CAD4 computer-controlled κ-axis diffractometer equipped with a graphite crystal, incident-beam monochromator. The cell constants and orientation matrix for data collection were obtained from a least-squares refinement method, using the setting angles of 25 reflections. Data were collected at r.t. using the ω-scan technique. Three standard reflections were monitored every hour, but no intensity variations were monitored. Lorentz and polarization corrections were applied to the data; however, no correction was made for absorption. The structure was solved by direct methods using SHELXS-86 [7] and refined by full-matrix least-squares calculations with SHELXL-97 [8]. Three non-coordinating methanol sites were identified, one of which was disordered. All non-hydrogen atoms were refined anisotropically; all hydrogen atoms, except those of the disordered methanol, were allowed to ride on geometrically ideal positions with isotropic temperature factors 1.2 times those of the attached non-hydrogen atoms. Crystal and intensity data are given in Table 1.

2.5. Electrochemical experiments

The working electrode was a glassy carbon disk (GC, electrochemical area = 0.064 cm^2), freshly polished with activated aluminum oxide (150 mesh, 58 Å, Aldrich) before use. The area of a GC electrode was determined

by chronocoulometry. The potential was stepped from +0.40 to +0.10 V versus Ag/AgCl in a 1 mM $K_3Fe(CN)_6$ aqueous solution (1 M KCl, $D_{ox} = 7.63 \times 10^{-6}$ cm^2 s^{-1}) with a pulse width of 500 ms [9]. The reference and counter electrodes were Ag/AgCl (3 M KCl) and Pt plates, respectively. All the potentials mentioned in this paper were referenced to Ag/AgCl.

For anaerobic voltammetric measurements, Ar was purged through electrolyte media for at least 10 min until no O_2 redox pair was seen on cyclic voltammograms. It should be noted that this fact does not necessarily mean that the media is completely absent from O_2, but is electrochemically O_2 free. The anaerobic conditions were also maintained under an Ar blanket throughout the measurements. Otherwise, the media were saturated with pure O_2 in order to examine the effects of complex **1** on O_2 redox reactions. All the electrochemical measurements described in this study were carried out at r.t. using a BAS CV-50W with a conventional three-electrode configuration.

2.6. SOD activity assay

SOD activity measurement was performed using a modified method of the light- and riboflavin-driven hydroxylaminenitrate SOD assay described by Archibald [10]. The reaction was performed in 0.1 ml of 25 mM Tris–HCl buffer (pH 8.0) containing 1 mM EDTA. The reaction mixture contained 10 μM of FMN, 5 mM of hydroxylamine, and a varying amount (10.0–0.078 μg) of complex **1**. The reaction commenced under light illumination for 25 min and then 0.1 ml of 20 mM sulfanilic acid and 0.1 ml of 7 mM naphthyl amine, both in 4.2 M acetic acid, were added to the reaction mixture. After standing for 20 min at r.t., the absorbance was measured at 540 nm with a microplate reader.

Table 1
Crystal data and structure refinement for **1**

Formula	$C_{27}H_{33}Cl_3FeN_7O_7$
F_W	729.80
Crystal system	triclinic
Space group	$P\bar{1}$
Unit cell dimensions	
a (Å)	10.143(2)
b (Å)	12.138(2)
c (Å)	13.937(2)
α (°)	90.97(2)
β (°)	109.77(1)
γ (°)	96.82(2)
V (Å^3)	1600.3(5)
Z	2
D_{calc} (g cm^{-3})	1.515
Absorption coefficient (mm^{-1})	0.777
Crystal size (mm)	0.60 × 0.45 × 0.10
θ Range for data collection (°)	1.56–22.47
No. independent reflections	4140
GOF on F^2	1.134
Final R indices [$I > 2\sigma(I)$][a]	$R_1 = 0.0694$, $wR_2 = 0.1592$
R indices (all data)	$R_1 = 0.1137$, $wR_2 = 0.1717$
Largest difference peak, hole (e Å^{-3})	0.380, −0.300

[a] $R_1 = \Sigma||F_o| - |F_c||/\Sigma|F_o|$ and $wR_2 = [\Sigma w(F_o^2 - F_c^2)^2/\Sigma wF_o^4]^{1/2}$.

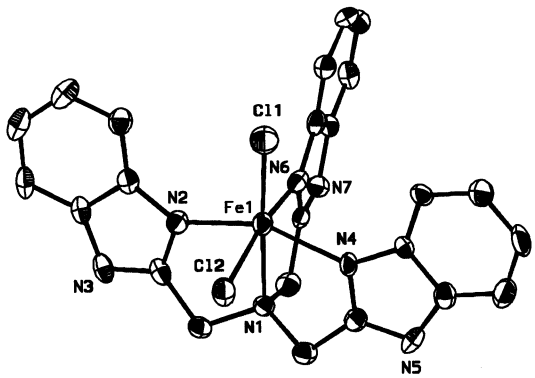

Fig. 1. ORTEP drawing of the $[Fe(ntb)Cl_2]^+$ (**1**).

3. Results and discussion

3.1. Preparation and characterization of complex *1*

$[Fe(ntb)Cl_2]ClO_4$ (**1**) can be synthesized using ferric chloride as a metal source and tris(2-benzimidazolylmethyl)amine as a neutral tripodal tetradentate ligand. For crystallization, perchlorate was used as a counter anion. The magnetic moment of complex **1** at r.t., 6.02 μ_B, corresponds to the spin-only value of high spin d^5 Fe(III), 5.92 μ_B. The DMF solution of complex **1** in a glycerol matrix gave a peak at m/z 498 in the FAB mass spectrum. This peak corresponds to the five-coordinate metal complex ion, $[Fe(ntb)Cl–H]^+$.

The paramagnetically-shifted ^{1}H NMR spectrum of complex **1** in DMSO-d_6 gave only three bands at 28.0, 44.2, and 64.2 ppm. The D_2O exchange experiment suggested that the band at 44.2 ppm is due to the amine protons of the benzimidazole groups. The remaining bands were tentatively assigned as benzyl protons. It is interesting that although there are two types of benzimidazole groups, only one type of amine proton is observed.

3.2. Molecular structure of complex *1*

An ORTEP drawing of complex **1** is shown in Fig. 1. Complex **1** is a *cis*-dichloro distorted octahedral complex. Three benzimidazole groups of ntb and a chloride anion formed the base of the octahedral geometry. One of the two axial positions was occupied by an apical nitrogen of ntb and the other site was occupied by another chloride anion. Two chloride anions in complex

1 are in a *cis* geometry, while the perchlorate anion exists as a counter ion. In the manganese complexes of the same ntb ligand, both trigonal bipyramidal geometry [6,11] and distorted octahedral geometry [11] were observed. However, only the distorted octahedral iron complex was observed in this study.

The average bond distance between the ferric ion and the two basal nitrogen atoms of the benzimidazole groups at the *cis* position of the basal chloride (2.093 Å) is about 0.04 Å shorter than that of the corresponding benzimidazole group at the *trans* position of the basal chloride (2.131 Å). The bond distance between the ferric ion and the basal chloride is 2.348 Å, whereas the distance between the ferric ion and the chloride anion at the *trans* position of the apical nitrogen is 2.214 Å. The bond distance between the ferric ion and the apical nitrogen atom (N1) of 2.332 Å is about 0.23 Å longer than the bond distances between the ferric ion and the basal nitrogen atoms of the benzimidazole groups (Table 2). A similar elongation is also observed in the other iron [12] and cobalt [13] complexes of tripodal tetradentate ligands containing a benzimidazolylmethyl group. However, this elongation is relatively shorter than that of the corresponding manganese [13b,14] and zinc [15] complexes. The average Fe–N_{bezim} distance of 2.093 Å is the same as that of the Fe–N_{im} distance of a high spin Fe(III) complex [3b,16] but is about 0.04 Å shorter than that of the Fe–N_{py} distance of a high spin Fe(III) complex [17]. The average bond distance suggests that the donor ability of the benzimidazole group is similar to that of imidazole group but is slightly better than that of the pyridine group.

3.3. Electrochemistry

A cyclic voltammetry investigation of a 5 mM complex **1**/0.1 M $TEABF_4$/DMF solution, performed under anaerobic conditions, indicated that Fe(III)/Fe(II) redox reactions are chemically reversible and occur at $+0.25$ V ($E_{1/2}$) (0.48 V versus NHE), as shown in Fig. 2. This value is a little higher than the optimal value of

Table 2
Bond lengths (Å) and angles (°) for **1**

Fe1–N1	2.332(6)	Fe1–N6	2.131(6)
Fe1–N2	2.091(6)	Fe1–Cl1	2.214(3)
Fe1–N4	2.095(6)	Fe1–Cl2	2.348(3)
N1–Fe1–N2	74.8(2)	N2–Fe1–Cl2	89.7(2)
N1–Fe1–N4	74.6(2)	N4–Fe1–N6	86.8(2)
N1–Fe1–N6	77.6(2)	N4–Fe1–Cl1	105.7(2)
N1–Fe1–Cl1	174.5(2)	N4–Fe1–Cl2	89.2(2)
N1–Fe1–Cl2	88.4(2)	N6–Fe1–Cl1	96.9(2)
N2–Fe1–N4	149.4(2)	N6–Fe1–Cl2	166.0(2)
N2–Fe1–N6	86.9(2)	Cl1–Fe1–Cl2	97.1(1)
N2–Fe1–Cl1	104.8(2)		

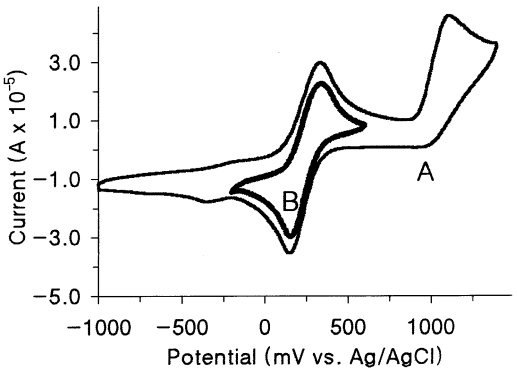

Fig. 2. Cyclic voltammograms of a 5 mM complex **1**/0.1 M $TEABF_4$/DMF solution, scanned at 100 mV s^{-1} within a wide (A) and a narrow (B) potential window. A solution was Ar purged and measurements were carried out under an Ar blanket.

≈ 0.36 V (versus NHE) and the values of 0.2–0.4 V observed in most Fe- and Mn-SODs [18]. The anodic to cathodic peak separation is 197 mV at 100 mV s^{-1} and increases with scan rates (not shown), indicating that the process deviates from a kinetic reversibility of 59 mV [19], and the electron transfer at the electrode surface is relatively slow. This renders the whole Fe(III)/Fe(II) electron transfer process quasi-reversible. Fig. 2(A) also shows that the complete irreversible oxidation of the complex occurs at $+1.1$ V, corresponding to the oxidation of benzimidazole rings. It should be noted that no dissolved-O_2 reduction wave was observed during the scan at more negative potentials than -1.2 V. This suggests that the medium is electrochemically free of dissolved O_2. The voltammogram exhibits a small hump at ca. -0.3 V during scans to a negative direction. This may be due to a small amount of impurity in the sample because its intensity does not change either under dioxygen purging or prolonged argon purging.

Rodriguez et al. investigated the electrochemical behavior of Fe(III) complexes with (bis[(1-methylimidazol-2-yl)methyl]amino)acetate ligands (L) in DMF and they reported that Fe^{II}–O_2 is oxidized at ca. 0.5 V lower potentials than the Fe(II) complex [3b]. They also observed that two Fe(III) reduction processes exist and two overlapping peaks become more distinct as scan rates increase. They claimed that one process results from the reduction of a complex with DMF as a ligand, while the other wave is responsible for the reduction of $Fe^{III}(L)Cl_2$. In our studies, complex **1** shows only a single reduction wave at ca. 0.2 V, and this is the case at higher scan rates, indicative of no Cl^- substitution with DMF. The substitution of the anionic chloride with the neutral DMF solvent might not be so easy because complex **1** is already monocationic.

In order to investigate the reaction of complex **1** with electrochemically generated superoxide, cyclic voltam-

metry of an O_2 saturated solution of 0.1 M complex **1**/DMF, containing no complex **1**, was first performed and compared to the result of a 5 mM solution of complex **1**. While Fig. 3(A) shows a redox pair at ca. -0.7 V due to O_2 reduction and O_2^- reoxidation, the O_2^- reoxidation wave completely disappears in a solution of complex **1** (Fig. 3(B)). This suggests that O_2^- electrochemically generated at the electrode surface reacts with complex **1** (reduced Fe(II) complex either/or oxidized Fe(III) complex) and transforms into an inert form for reoxidation. It should be noted that the appearance of an O_2^- reoxidation wave depends on the concentration of complex **1** and the scan rate, indicating that the reaction of O_2^- with complex **1** is relatively slow within an experimental time scale. We confirmed that the O_2^- reoxidation wave begins to be seen in solutions of 1 mM or lower concentrations of complex **1** when scanned at 100 mV s^{-1}. This trend is also true when scanned faster than 500 mV s^{-1} in 5 mM solutions of complex **1**.

From the comparison of Fig. 3(A) and (B), other features can be drawn. First, the total charge passed during O_2 reduction in a solution containing complex **1** (Fig. 3(B)) is approximately twice the charge in a solution containing no complex **1** (Fig. 3(A)). Although it can be anticipated that simultaneous Fe(III) reduction during O_2^- generation will increase the cathodic current, it is only partially responsible for the increase in the total reduction current since the background current, due to continuous Fe(III) reduction, is relatively small, as shown in Fig. 3(A). If complex **1** behaves only as an O_2^- radical scavenger, the reduction current enhancement could not be explained fully. Fe-containing SOD disproportionates O_2^- by the following two-step reaction [1]:

$$Fe^{III}\ \text{complex} + O_2^- \rightarrow Fe^{II}\ \text{complex} + O_2$$

$$Fe^{II}\ \text{complex} + O_2^- \rightarrow Fe^{III}\ \text{complex} + O_2^{2-}$$

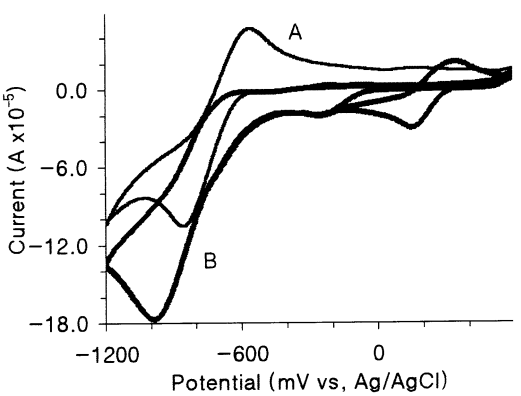

Fig. 3. Cyclic voltammograms of O_2 saturated solutions of 0.1 M $TEABF_4$/DMF, containing no complex **1** (A) and 5 mM complex **1** (B), scanned at 100 mV s^{-1}. A solution was O_2 purged and measurements were carried out under an O_2 blanket.

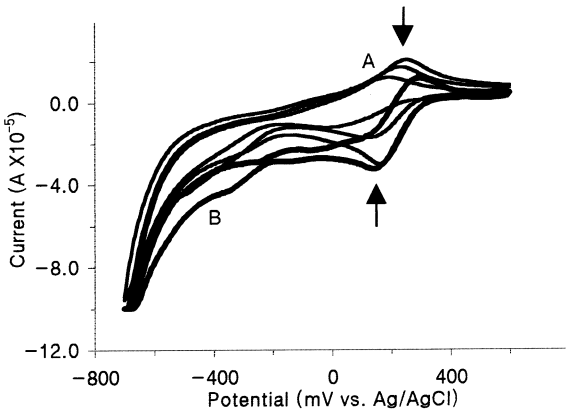

Fig. 4. Cyclic voltammograms of an O_2 saturated solution of 5 mM complex **1**/0.1 M $TEABF_4$/DMF, scanned at 100 mV s^{-1}. The potential was scanned between -0.7 and $+0.6$ V under stationary (A) and hydrodynamic (B) conditions. A series of curves in (A) indicates the 2nd, 11th, and 20th scans.

The reduction current enhancement could occur through either the increase of O_2 concentration at the electrode surface by the first reaction or the increase of the Fe(III) concentration at the electrode surface by the second reaction, or through both reactions. The result appears to indicate catalytic effects of complex **1**. Second, the Fe(III)/Fe(II) redox wave, shown during an initial potential scan in Fig. 3(B) (the cycling was started at -0.2 V and scanned toward a positive potential limit), disappears once the superoxide radical is generated at the electrode surface. However, the O_2 reduction wave reaches a steady-state value and is not reduced during continuous cycling. The same behavior can be obtained in a 5 mM complex **1**/0.1 M $TEABF_4$/DMSO solution. The steady-state cyclic voltammogram, cycled between -0.2 and $+0.6$ V at 100 mV s^{-1}, indicates no suppression of Fe(III)/Fe(II) redox. The wave characteristics are the same as those in Fig. 2(B); it is reasonable to speculate that reaction of complex **1** with O_2^- finally leads to electrode surface deterioration. This reasoning was further investigated under hydrodynamic voltammetry conditions. The solution was slowly stirred and a cyclic voltammogram was obtained simultaneously. Fig. 4 compares cyclic voltammograms in stationary (A) and hydrodynamic (B) conditions. When the solution is potential-cycled in between -0.7 and $+0.6$ V without stirring, the decrease of Fe(III)/Fe(II) redox wave can be visualized since O_2^- generation is minimal at -0.7 V. Three curves in Fig. 4(A) correspond to the 2nd, 11th, and 20th cycles in a decreasing order. Meanwhile, the reactants and products move rapidly into and out of the electrode surface under hydrodynamic conditions, leading to alleviation of the surface fouling effect as shown in Fig. 4(B).

It is quite surprising that the electrode surface deterioration does not affect electron transfer behavior between the electrodes and O_2, and the O_2^- scavenging

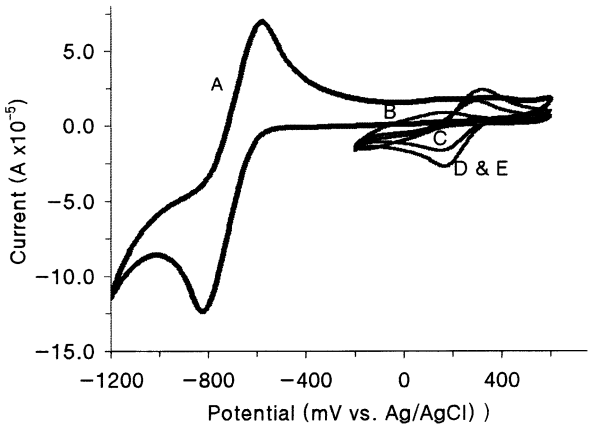

Fig. 5. Cyclic voltammograms of the electrode, after maintaining at −1.1 V for 10 min in a 5 mM complex **1**/0.1 M $TEABF_4$/DMF solution, in a 0.1 M $TEABF_4$/DMF solution (A) and a 5 mM complex **1**/0.1 M $TEABF_4$/DMF solution (B–E). All the solutions were O_2 saturated and measurements for (B–E) were obtained immediately after (A). (B–E) correspond to 2nd, 10th, 20th, and 30th scans.

effect. After being maintained at −1.1 V for 10 min in a 5 mM complex **1**/0.1 M $TEABF_4$/DMF solution, the electrode was immediately immersed in a complex **1**-free solution and potential-cycled. Prior to each step, the solutions were saturated with O_2 and the electrochemical measurements were performed under an O_2 blanket. Fig. 5(A) demonstrates the O_2 redox processes in a complex **1**-free solution. It should be pointed out that the cyclic voltammetry results (peak heights and areas) are quite similar to Fig. 3(A), indicating that the O_2 redox process is not prohibited by electrode surface deterioration. This result supports the fact that complex **1** still plays a role as a superoxide scavenger, while the Fe(III)/Fe(II) redox reaction is suppressed, corresponding to the result shown in Fig. 3(B). The surface-fouled electrode was placed back into a 5 mM complex **1**/0.1 M $TEABF_4$/DMF solution and cycled continuously between −0.2 and +0.6 V. Fig. 5(B–E) shows that the Fe(III)/Fe(II) redox process slowly recovers and finally attains a diffusion-controlled cyclic voltammogram.

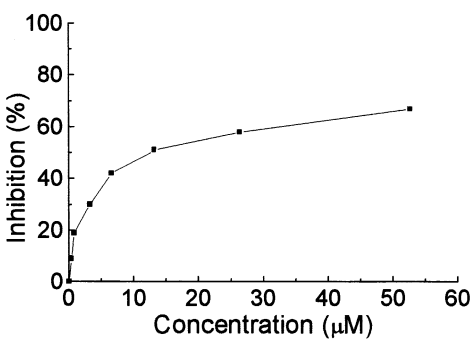

Fig. 6. SOD activity of complex **1** in the light- and riboflavin-driven hydroxylaminenitrate SOD assay method.

3.4. SOD activity assay

We examined the SOD activity of complex **1** using a modified method of the light- and riboflavin-driven hydroxylaminenitrate SOD assay. Complex **1** inhibited the conversion of hydroxylamine to nitrate by O_2^-. The inhibition results are given in Fig. 6. The IC_{50} value is 13.3 μM and is an order of magnitude higher than that of the best activity recorded with a (benzoato)-manganese(II) complex [4e].

3.5. Reactivity

Reaction of complex **1** with one equivalent of O_2^- radical in methanol gave a μ-oxo iron complex $[Fe_2O(ntb)_2Cl_2](ClO_4)_2$ (**2**). The cation part of the complex **2**[1] is identical to the previously reported μ-oxo iron complex, $[Fe_2O(ntb)_2Cl_2](PF_6)_2$ [11a]. Interestingly, complex **2** could also be synthesized from complex **1** with acetate or hexamethylene diamine instead of an O_2^- radical. A superoxide radical might behave as a base in methanol. The reaction of complex **1** with an O_2^- radical as a base might be a competitive side-reaction and ultimately lead to a μ-oxo iron complex. The μ-oxo iron complex might be responsible for the electrode surface fouling.

In conclusion, we obtained a crystal structure of a mononuclear Fe(III) complex with a tripodal ligand ntb, where ntb served as a neutral tetradentate chelating ligand for a distorted octahedral ferric ion. The SOD activity of complex **1** was demonstrated using both a direct observation of O_2^- decay using cyclic voltammograms and an indirect inhibition method. It is interesting that a manganese(II) complex, synthesized using the same ligand, showed no SOD activity at all [6], while complex **1** showed SOD activity. It is not surprising that the SOD activities are strongly dependent on the redox potentials of the metal ion [18]. With the exception of so-called cambiolistic SODs, Fe-sub-(Mn)SODs (or Mn-sub-(Fe)SODs) have no catalytic activities. The redox potential of complex **1** is 0.48 V (versus NHE) in DMF, while the corresponding manganese(II) complex is redox inactive at the DMF window. To improve the activity of the SOD mimics, we need to reduce the redox potentials of the complex.

[1] Crystallographic data for **2**: triclinic, $P\bar{1}$, $a = 12.036(4)$, $b = 12.838(2)$, $c = 13.637(3)$ Å, $\alpha = 63.49(2)$, $\beta = 67.90(3)$, $\gamma = 79.31(2)°$, $V = 1746.7(7)$ Å^3, $Z = 2$, $D_{calc} = 1.339$ g cm^{-3}. Final R factors were $R_1 = 0.083$ and $wR_2 = 0.2386$ for 3886 reflections.

4. Supplementary material

Tables giving a structural determination summary, atomic coordinates, temperature factors, bond lengths, bond angles, and anisotropic thermal parameters for non-hydrogen atoms and atomic coordinates for hydrogen atoms, F_o/F_c tables, and ORTEP drawings with complete atomic numbering for **1** and **2** are available from the authors upon request.

Acknowledgements

We thank the Korean Institute of Basic Science for elemental and mass spectroscopy analyses, and the National Institute of Technology and Quality for the use of an X-ray diffractometer. The authors wish to acknowledge the financial support of the Korea Research Foundation (Grant No. 98-O15-D00142) and Hanyang University (1999).

References

[1] (a) I. Fridovich, Annu. Rev. Biochem. 64 (1995) 97. (b) I. Fridovich, J. Biol. Chem. 264 (1989) 7761.
[2] J.-L. Pierre, P. Chautemps, S. Refaif, C. Beguin, A.E. Marzouki, G. Serratrice, E. Saint-Aman, P. Rey, J. Am. Chem. Soc. 117 (1995) 1965 and Refs. therein.
[3] (a) D. Zhang, D.H. Busch, P.L. Lennon, R.H. Weiss, W.L. Neumann, D.P. Riley, Inorg. Chem. 37 (1998) 956. (b) M. Rodriguez, I. Morgenstern-Badarau, M. Cesario, J. Guilhem, B. Keita, L. Nadjo, Inorg. Chem. 35 (1996) 7804. (c) W.S. Szulbinski, P.R. Warburton, D.H. Busch, Inorg. Chem. 32 (1993) 5368. (d) L. Iluliano, J.Z. Pedersen, A. Ghiselli, D. Pratico, G. Rotilio, F. Violi, Arch. Biochem. Biophys. 293 (1992) 153. (e) T. Nagano, T. Hirano, M. Hirobe, Free Radical Res. Commun. 12 (1991) 221. (f) M. Farragi, P. Peretz, D. Weinraub, Int. J. Radiat. Biol. 49 (1986) 951. (g) C. Bull, G.J. McClune, J.A. Fee, J. Am. Chem. Soc. 105 (1983) 5290.
[4] (a) D.P. Riley, P.J. Lennon, W.L. Neumann, R.H. Weiss, J. Am. Chem. Soc. 119 (1997) 6522. (b) D.P. Riley, S.L. Henke, P.J. Lennon, R.H. Weiss, W.L. Neumann, W.L. Rivers, K.W. Aston, K.R. Sample, H. Rahman, C.-S. Ling, J.-J. Shieh, D.H. Busch, W. Szulbinski, Inorg. Chem. 35 (1996) 5213. (c) R. Rajan, R. Rajaram, B.U. Nair, T. Ramasami, S.K. Mandal, J. Chem. Soc., Dalton Trans. (1996) 2019. (d) A. Deroche, I. Morgenstern-Badarau, M. Cesario, J. Guihem, B. Keita, L. Nadjo, C. Houée-Levin, J. Am. Chem. Soc. 118 (1996) 4567. (e) D.P. Riley, R.H. Weiss, J. Am. Chem. Soc. 116 (1994) 387. (f) N. Kitajima, M. Osawa, N. Tamura, Y. Moro-oka, T. Hirano, M. Hirobe, T. Nagano, Inorg. Chem. 32 (1993) 1879. (g) R.H. Weiss, A.G. Flickinger, W.J. Rivers, M.M. Hardy, K.W. Aston, U.S. Ryan, D.S. Riley, J. Biol. Chem. 268 (1993) 23049. (h) Y. Nishida, I. Watanabe, K. Unoura, Chem. Lett. (1991) 1517. (i) B.H.J. Bielski, P.C. Chan, J. Am. Chem. Soc. 100 (1978) 1920. (j) J.S. Valentine, A.E. Quinn, Inorg. Chem. 15 (1976) 1997.
[5] M.S. Lah, M.M. Dixon, K.A. Pattridge, W.C. Stallings, J.A. Fee, M.L. Ludwig, Biochemistry 34 (1995) 1546.
[6] M.S. Lah, H. Chun, Inorg. Chem. 36 (1997) 1782.
[7] G.M. Sheldrick, Acta. Crystallogr., Sect. A 46 (1990) 467.
[8] G.M. Sheldrick, SHELXL-97, University of Göttingen, Germany, 1997.
[9] M. Freund, L. Bodalbhai, A. Brajter-Toth, Talanta 38 (1991) 95.
[10] F.S. Archibald, Methods in Enzymology, Oxygen Radicals in Biological Systems, Part B, vol. 186, Academic Press, New York, 1990, pp. 237–241.
[11] A.R. Oki, P.R. Bommarreddy, H. Zhang, N. Hosmane, Inorg. Chim. Acta 231 (1995) 109.
[12] (a) R.M. Buchanan, R.J. O'Brien, J.F. Richardson, J.-M. Latour, Inorg. Chim. Acta 214 (1993) 33. (b) S. Wang, Q. Luo, X. Wang, L. Wang, K. Yu, J. Chem. Soc., Dalton Trans. (1995) 2045.
[13] (a) M.S. Lah, M. Moon, Bull. Korean Chem. Soc. 18 (1997) 406. (b) K. Takahashi, Y. Nishida, S. Kida, Bull. Chem. Soc. Jpn. 57 (1984) 2628.
[14] K. Takahashi, Y. Nishida, S. Kida, Inorg. Chim. Acta 77 (1983) L185.
[15] (a) U. Hartmann, R. Gregorzik, H. Vahrenkamp, Chem. Ber. 127 (1994) 2123. (b) R. Gregorzik, U. Hartmann, H. Vahrenkamp, Chem. Ber. 127 (1994) 2117.
[16] M. Rodriguez, F. Lambert, I. Morgenster-Badaru, M. Cesario, J. Guilhem, B. Keita, L. Nadjo, Inorg. Chem. 36 (1997) 3525.
[17] (a) T. Kojima, R.A. Leising, S. Yan, L. Que Jr., J. Am. Chem. Soc. 115 (1993) 11328. (b) D.D. Cox, L. Que Jr., J. Am. Chem. Soc. 110 (1988) 8085. (c) Y. Dong, H. Fujii, M.P. Hendrich, R.A. Leising, G. Pan, C.R. Randall, E.C. Wilkinson, Y. Zang, L. Que Jr., B.G. Fox, K. Kauffmann, E. Münck, J. Am. Chem. Soc. 117 (1995) 2778. (d) Y. Zang, Y. Dong, L. Que Jr., J. Am. Chem. Soc. 117 (1995) 1169. (e) Y. Zang, G. Pan, L. Que Jr., J. Am. Chem. Soc. 116 (1994) 3653. (f) E.C. Wilkinson, Y. Dong, L. Que Jr., J. Am. Chem. Soc. 116 (1994) 8394.
[18] C.K. Vance, A.-F. Mikker, J. Am. Chem. Soc. 120 (1998) 461.
[19] A.J. Bard, L.R. Faulkner, Electrochemical Methods, Wiley, New York, 1980.